The Dynamics of Ligand Barrier Crossing inside the Acetylcholinesterase Gorge

Jennifer M. Bui*, Richard H. Henchman*, and J. Andrew McCammon*†
*Howard Hughes Medical Institute, Department of Chemistry and Biochemistry; and †Department of Pharmacology, University of California San Diego, La Jolla, California 92093-0365

ABSTRACT The dynamics of ligand movement through the constricted region of the acetylcholinesterase gorge is important in understanding how the ligand gains access to and is released from the active site of the enzyme. Molecular dynamics simulations of the simple ligand, tetramethylammonium, crossing this bottleneck region are conducted using umbrella potential sampling and activated flux techniques. The low potential of mean force obtained is consistent with the fast reaction rate of acetylcholinesterase observed experimentally. From the results of the activated dynamics simulations, local conformational fluctuations of the gorge residues and larger scale collective motions of the protein are found to correlate highly with the ligand crossing.

INTRODUCTION

The fast hydrolysis rate (Quinn, 1987) of acetylcholinesterase (AChE) to terminate the activity of the cationic neurotransmitter acetylcholine (ACh) still remains an unresolved topic of interest. The enzyme architecture with the catalytic triad at the bottom of the 20-Å deep and narrow gorge seen in the crystal structures (Bourne et al., 1995; Sussman et al., 1991) runs counter to the properties expected for the fast rate. In particular, ACh would have to push past the many bulky aromatic side chains that are spaced too close to allow its free passage to and from the active site. Several computational studies have attempted to consider the mechanisms by which substrates bind or products are released from AChE (Enyedy et al., 1998; Malany et al., 1999; Wlodek et al., 1997). Molecular dynamics (MD) simulations (Gilson et al., 1994; Tai et al., 2002; Wlodek et al., 2000; Zhou et al., 1998) provide substantial evidence that the gorge exists in two states, closed and open. It was also found that AChE favored the closed state in which the radius of the bottleneck was too small to allow substrate to cross. Both theoretical and experimental studies (Antosiewicz et al., 1996; Faerman et al., 1993; Gilson et al., 1994; Malany et al., 1999; Ripoll et al., 1993; Tan et al., 1993; Wlodek et al., 2000) have shown that the charge distribution of the enzyme creates an electric field that helps to accelerate the rate of binding of a positively charged ligand into the active site, although the same effect would also hinder ligand exit.

A complete understanding of how the substrate actually binds and how charged products of the hydrolysis reaction are released must be based on a detailed knowledge of the reaction dynamics. In this work, the dynamics of tetramethylammonium (TMA) crossing the bottleneck region of the gorge are examined. TMA is an appropriate choice of ligand to probe the binding dynamics of the enzyme, for the TMA resembles the bulkiest part of ACh. Like ACh, the TMA is a quaternary ammonium ion. Using umbrella potential sampling, the free energy profile of the TMA passage through the bottleneck region of the enzyme is computed and the peak of the potential barrier is located in the constricted region. Multiple MD trajectories of the TMA crossing the potential barrier are simulated using the activated dynamics techniques (McCammon and Harvey, 1987) to investigate the dynamics of the bottleneck region as the TMA passes through.

Submitted April 18, 2003, and accepted for publication July 3, 2003.

Address reprint requests to Jennifer Bui, E-mail: jbui@mccammon.ucsd.edu.

0006-3495/03/10/2267/06 $2.00

METHODS

System setup and MD equilibration

From the 10-ns molecular dynamics simulation study of AChE by Tai et al. (Tai et al., 2001), a snapshot with a large gorge opening was chosen as the starting configuration. The TMA ligand was placed in the bottleneck region between the aromatic rings of residues Y124 and F338. The ligand was positioned with the nitrogen atom (center atom of the TMA) at the midpoint between the α-carbons of Y124 and F338. To create free volume for inserting the TMA into the bottleneck region, three water molecules in this region were removed. The atoms within 10 Å of the center atom of the TMA were then equilibrated for 10 ps to relax the ligand and surrounding atoms under the same MD simulation conditions that were used in the 10-ns molecular dynamics simulation study of AChE by Tai, et al. (Tai et al., 2001). The whole system was then equilibrated and velocities were reassigned from a 300 K Maxwellian distribution every 1 ps for a 5-ps period using NWChem 4.0 molecular dynamics software (Straatsma et al., 2000), and the Amber 95 force field (Cornell et al., 1995). Full details are provided in the publication by Tai et al. (2001).

Generating a representative collection of configurations at the bottleneck region using umbrella sampling

To compute the potential of mean force (PMF) of the TMA through the constricted region of the gorge, the reaction coordinate, δ, was defined as the distance from the center of mass of the whole enzyme to the nitrogen atom of the ligand. The steric restraints due to the protein atoms align the reaction coordinate with the axis of the gorge. The center of mass of the enzyme was chosen as the origin of the reaction coordinate because this point provides a stable reference point, as opposed to any single atom in the system, and because the center of mass of the enzyme is very close to the active site residue S203. A harmonic restraining potential, $U(\delta)$, with the force

constant, k, of 50 kJ mol^{-1} Å^{-2} was used to confine the TMA in each window,

$$U(\delta) = k(\delta - \delta_0)^2,$$

where δ is the restraint distance as defined above. Seven windows were placed along the reaction coordinate at 0.6-Å intervals from $\delta = 9.9$–13.5 Å. For each window, 1.0 ns of dynamics sampling was performed. The PMF was computed from the probability distribution, $\rho(\delta)$, of the TMA along the reaction coordinate (Kottalam and Case, 1988; McCammon and Harvey, 1987)

$$\rho(\delta) = \frac{\int e^{-\beta V} d\Sigma}{\int e^{-\beta V} d\delta\, d\Sigma},$$

where $\beta = (k_b T)^{-1}$, k_b is the Boltzmann constant and T is temperature. $d\Sigma$ represents the spatial coordinates of all the atoms in the system except the component along the reaction coordinate, and V is the total potential energy of the system. The measured distribution, $\rho^*(\delta)$, in the presence of the harmonic restraint potential, $U(\delta)$, is related to $\rho(\delta)$ by

$$\begin{aligned}\rho^*(\delta) &= e^{-\beta U(\delta)} \frac{\int e^{-\beta V} d\Sigma}{\int e^{-\beta(V+U)} d\delta\, d\Sigma} \\ &= e^{-\beta U(\delta)} \frac{\int e^{-\beta V} d\Sigma}{\int e^{-\beta V} d\delta\, d\Sigma} \frac{\int e^{-\beta V} d\delta\, d\Sigma}{\int e^{-\beta(V+U)} d\delta\, d\Sigma}. \\ &= e^{-\beta U(\delta)} \rho(\delta) / \langle e^{-\beta U} \rangle\end{aligned}$$

The probability distribution, $\rho(i)$, of δ values for each window was determined using a 0.1-Å bin width. To form a continuous distribution of the ligand, consecutive windows were pieced together by the method of Shen et al. (Shen and McCammon, 1991). First the scaling factor, S, was determined using the following expression:

$$\sum_i [\rho_1(i) - S\rho_2(i)][n_1(i)n_2(i)]^2 = 0,$$

where $\rho_1(i)$ is the more densely sampled distribution that overlapped with the adjacent distribution, $\rho_2(i)$, and $n_j(i)$ is the number of times that δ was found in the i^{th} bin for the j^{th} distribution. Once S was determined, the two probability distributions were merged into an extended distribution using the following expression:

$$\rho(i) = \frac{\rho_1(i)n_1(i) + S\rho_2(i)n_2(i)}{n_1(i) + n_2(i)}.$$

Finally, the PMF, $W(\delta)$, of the TMA was obtained from

$$W(\delta) = -k_b T \ln(\rho(\delta)) + C,$$

where $C = -k_b T \ln\langle \exp(-\beta U) \rangle$ is a constant that links the two adjacent windows together.

Forward and reversed trajectories

A set of different phase space points within the bottleneck region was chosen from the above umbrella sampling simulations as the initial phase space points for studying the dynamics of barrier crossing. Trajectories were run from these phase space points in the absence of the harmonic potential. To avoid any artifacts due to the removal of the harmonic potential, phase space points that had zero restraint potential were selected as the starting points (Wong et al., 1993). The trajectories were propagated once with the velocities of all atoms in the initial states generated by umbrella sampling and once with the negative of these velocities. Since the equations of motion of classical mechanics are symmetric in time, the trajectories can be propagated forward and backward in time to generate a representative set of barrier transitions (McCammon and Harvey, 1987). The trajectory with the original velocities is called the forward trajectory and the trajectory obtained using the initial velocities with the opposite sign is called the reversed trajectory. The reversed trajectory can be reordered in time and appended to the start of the forward trajectory to give one full trajectory of an attempted crossing of the barrier.

RESULTS AND DISCUSSION

Potential of mean force in the bottleneck region

The parabolic umbrella potentials that constrain the TMA in each window along the reaction coordinate are illustrated in Fig. 1 *A*. The distribution of δ values in the bins of width 0.1 Å are shown in Fig. 1 *B*. The TMA distributions did not adequately overlap between the window at $\delta = 11.1$ Å and the window at $\delta = 11.7$ Å. Therefore, an additional window was placed in between at $\delta = 11.4$ Å with a force constant twice as large, 100 kJ mol^{-1} Å^{-2}, to restrain the TMA in this bin. From the distributions of the TMA along the reaction coordinate, the PMF of the system in this bottleneck region was computed using the method described above (Fig. 1 *C*). The PMF calculations using distributions of δ values for each window of different bin widths (0.1–0.3 Å) were also computed. The relative values of PMFs of the TMA through the constricted region were not highly dependent on the grid elements. The peak of the PMF barrier was at 11.3 Å from the center of mass of the enzyme and located in the

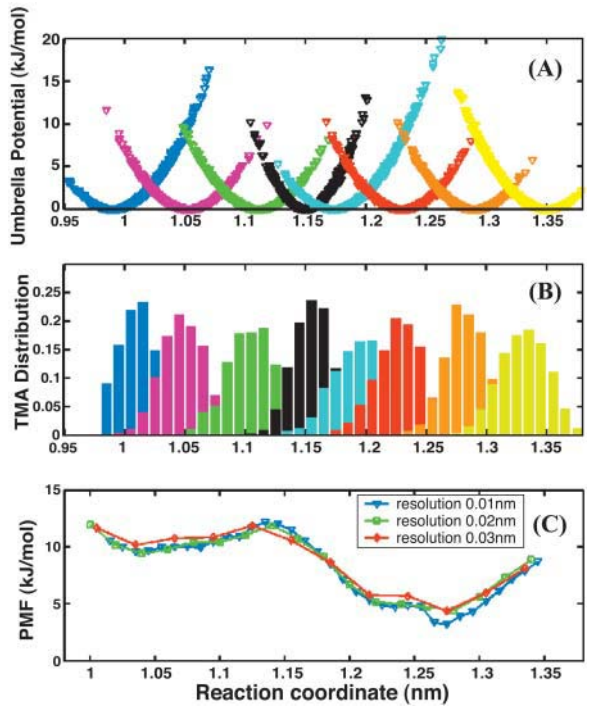

FIGURE 1 (*A*) The umbrella restraint potentials with force constant $k =$ 50 kJ mol^{-1} Å^{-2} except for window # 4, $k = 100$ kJ mol^{-1} Å^{-2}. (*B*) The probability distribution of δ values for each window, for a 0.1-Å bin width. (*C*) PMF, for different resolutions of the grid elements.

bottleneck region. From this energy profile, the incoming ligand has to cross an energy barrier of 8–10 kJ mol^{-1} to reach the active site of the enzyme. Contrary to what might be expected from the narrow bottleneck seen in the static crystal structures, the barrier for the incoming ligand is surprisingly low. The constricted region of the gorge lined with many bulky aromatic side chains seems to hinder the motion of the charged ligand only slightly. The aromatic side chains appear to move aside, facilitating the entry of the TMA. As will be seen in the next section, the low energy barrier is consistent with the fast reaction rate of the AChE observed experimentally.

Estimation of the barrier-crossing rate constant

Once the free energy profile of the TMA in the bottleneck region has been determined, the kinetic rate constant, k, of passage over the barrier can be obtained from reaction rate theory (Case, 1993; McCammon and Harvey, 1987). Since the motion of the TMA along the reaction coordinate is in the high friction regime, the Kramers modified transition state theory (TST) (Hanggi et al., 1990; Marrink and Berendsen, 1996; Roux and Karplus, 1991a,b) was used to calculate k using the expression

$$k = \kappa_{\text{Kramers}} \frac{\omega_i}{2\pi} e^{-\Delta E_o/RT},$$

where $\kappa_{\text{Kramers}} = (m\omega_b/\varsigma)$ is the transmission coefficient, m is the mass of the ligand, ζ is the friction coefficient, ${\omega_b}^2 = W''(\delta_b)/m$ is the squared frequency of crossing at the barrier peak (Marrink and Berendsen, 1996), δ_b, and $W''(\delta_b)$ is the second derivative of the PMF at δ_b . The quantity ω_i is the angular frequency of oscillation associated with the initial well. Using the gorge water friction coefficient estimated from the 10-ns MD simulation of apo-AChE, the transmission coefficient, κ_{Kramers}, was estimated by Stokes scaling to be 0.17. This low value is expected for this overdamped protein reaction (Northrup et al., 1982). The TMA crossed the barrier top many times (Fig. 2), which is consistent with the dynamics of barrier crossing in the high frictional regime. ω_i for the incoming ligand is $\sim 10^{11}$ s^{-1}. For the barrier height of 8 kJ/mol, the rate constant, k, for the incoming ligand would be 10^8 s^{-1}. This is a very high rate constant. It is of interest to relate this rate constant to the kinetics of substrate binding of AChE according to the reaction rate mechanism (Quinn, 1987) below:

$$[\text{AChE}] + [\text{S}] \underset{k_{-1}}{\overset{k_1}{\leftrightarrow}} [\text{AChE/S}] \underset{k_{-2}}{\overset{k_2}{\leftrightarrow}} [\text{AChE/S}]^{\#} \overset{k_3}{\rightarrow} \text{product}\ldots$$

Assuming k_3 is so fast that the steady state approximation might be applied to both [AChE/S] and $[\text{AChE/S}]^{\#}$, the effective forward constant, k_{eff}, can be approximated as $k_{\text{eff}} = (k_1k_2/k_{-1}+k_2)$. In addition, k_{-1} can also be estimated using the Stokes law with the gorge viscosity. The first passage time for the TMA to travel away from the bottleneck region and escape to the bulk is $\sim 10^{-8}$s; this yields k_{-1} $\sim 10^8$ s^{-1}. Therefore, the rate of barrier crossing, k_2, is comparable to the reversed rate, k_{-1}. Hence, the effective rate of substrate binding to AChE is the rate at which substrate and enzyme encounter. That is, the enzyme operates in the diffusion controlled limit, which is consistent with experimental kinetic data (Quinn, 1987).

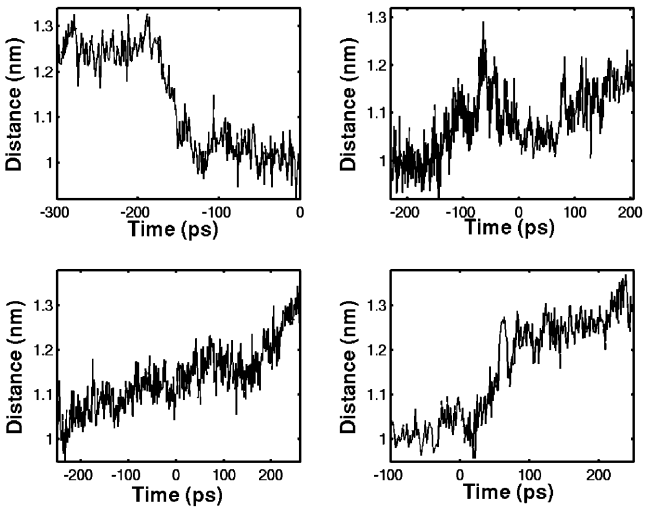

FIGURE 2 Successful crossing trajectories of the TMA over the barrier. The reversed trajectory is reordered in time and appended to the start of the forward trajectory to give one full trajectory. Only the crossing portion of each 600 ps successful trajectory is reported.

Dynamics of the gorge residues

The time forward and reversed trajectories, which were generated as described in the method section, allow studying of the unrestrained dynamics of barrier crossing of the TMA. Any trajectory in which the TMA moved from $\delta < 10.5$ Å on one side of the barrier to $\delta > 12.5$ Å on the other was called a successful crossing trajectory. Some successful trajectories are shown in Fig. 2. These successful trajectories exhibited the stochastic crossing behavior of the TMA in a high friction regime. It takes ~50–200 ps for the TMA to cross the barrier. Only a portion of the time forward and reversed trajectories resulted in successful crossing transitions due to the high damping friction, (12 full trajectories of 600 ps each were conducted; only four of them show successful crossing).

To observe the dynamics of the gorge residues in this bottleneck region that couple with the movement of the TMA, the distance the TMA travels was compared to the average distance between F338: C_α and Y124: C_α (Fig. 3). This distance was chosen because it had previously been seen to correlate highly with the gorge size in other MD studies (Tai et al., 2001; Zhou et al., 1998). (These references also present detailed examples of opening events and their frequency of occurrence.) As the TMA crosses this constriction region, the distance between F338: C_α and Y124: C_α

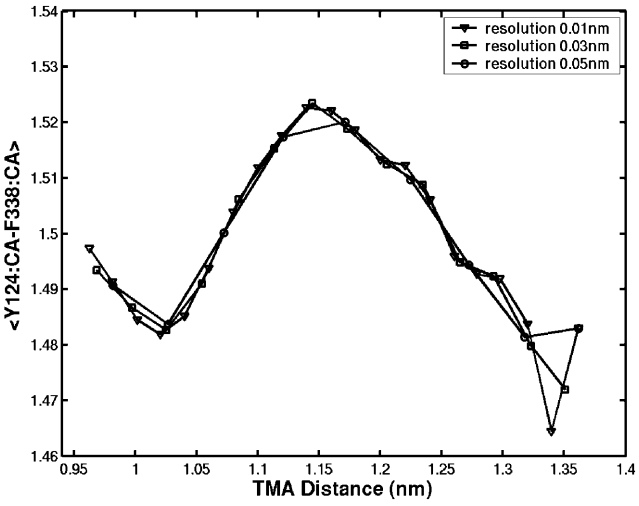

FIGURE 3 The correlation of the TMA distances with the average distances between F338:C_α and Y124:C_α. For each δ bin of different resolutions, the average distance between F338:C_α and Y124:C_α of the 12 full MD trajectories is computed.

increases until it reaches a maximum. Of considerable interest, this TMA position corresponds to the distance of the TMA at which the PMF is also maximal. This indicates that the backbones of these two gating residues move away from each other, widening the gorge and allowing the TMA to cross. The distance then relaxes to the original value when TMA passes over the barrier peak. To detect the gorge states, a probe of 2.5 Å in radius was used to roll around the van der Waals surface of the residues in the constricted region. If the 2.5-Å probe surface in the active site region is connected to that of the exterior, the gorge is open. When the TMA is at the barrier peak, it is found that the gorge opens to allow the TMA to cross. The surface is typically disconnected at the bottleneck before and after the TMA crosses. Movies of the gorge closing and opening are available at http://mccammon.ucsd.edu.

The movements of the aromatic side chains in this region are also highly correlated to motion of the TMA, as depicted in Fig. 4. Small fluctuations of these side chains to create room for the ligand crossing were observed. The D74 side chain flips to and fro forming hydrogen bonds with the Y124:OH and Y341:OH in response to the different positions of the ligand. The creation of the hydrogen bond of D74:OD and Y124:OH, which lifts up the side chain of Y124 in the direction of the gorge entrance, appears to help the TMA to pass the constricted zone. This supports the idea that D74 influences the movement of the cation inside the gorge (Hosea et al., 1996; Mallender et al., 2000; Radic et al., 1997). The side chains of residues Y337 and Y341 are significantly displaced as the TMA moved through the bottleneck region. The formation of the hydrogen bond of D74 and Y341 before and after the TMA crosses suggests a strong correlation of these side chains to facilitate the TMA passage through the bottleneck.

Not only were the breathing motions of the residues of the gorge highly correlated to the movements of the TMA, but correlated displacements on larger scales were also observed. To demonstrate the collective protein dynamics that contributes to the bottleneck opening, we defined the following correlation parameter:

$$C_i = \frac{\langle (R_i(t) - \langle R_i \rangle)(\xi_i(t) - \langle \xi \rangle) \rangle}{\sqrt{\langle (R_i(t) - \langle R_i \rangle)^2 \rangle \langle (\xi_i(t) - \langle \xi \rangle)^2 \rangle}},$$

where ξ is the distance between Y124: C_α and F338:C_α and R_i is the Cartesian coordinate of all of the C_α atoms of the enzyme residues. Three porcupine plots (Tai et al., 2001) of these correlation parameters that correspond to different positions of the TMA, precrossing (i.e., where the TMA was at $\delta = 10.0$ Å), transition ($\delta = 11.3$ Å), and postcrossing ($\delta = 13.5$ Å), are shown in Fig. 5. These plots show how the C_α atoms are displaced according to the TMA position relative to their average values taken over all of the 12 full MD trajectories. The color gradient from red, the most, to blue, the least, indicates the extent of correlation of each residue's motion to the gorge's width, ξ. The porcupine plot representation highlights the concerted

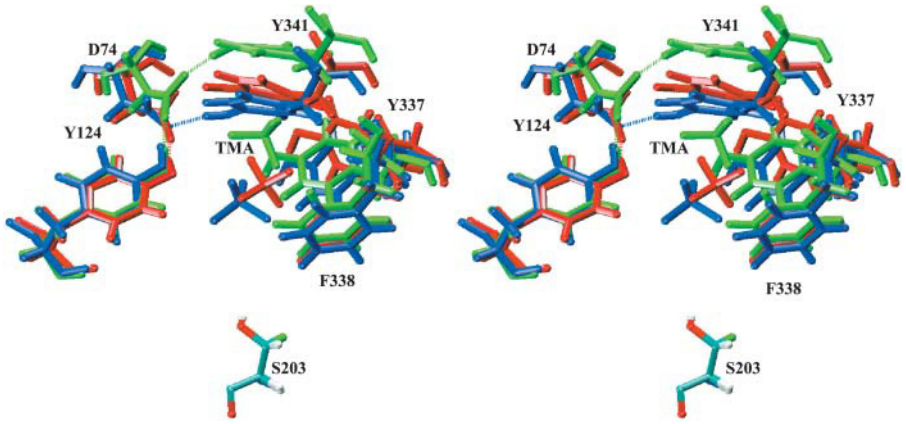

FIGURE 4 Stereo pictures of crossing dynamics in the bottleneck region are generated using VMD (Humphrey and Schulten, 1996). Blue, before the TMA crosses the barrier. Red, the TMA is at peak of the PMF. Green, after the TMA crosses the barrier. Dashed lines are the H-bonds. The crossed-eyes stereo convention is used.

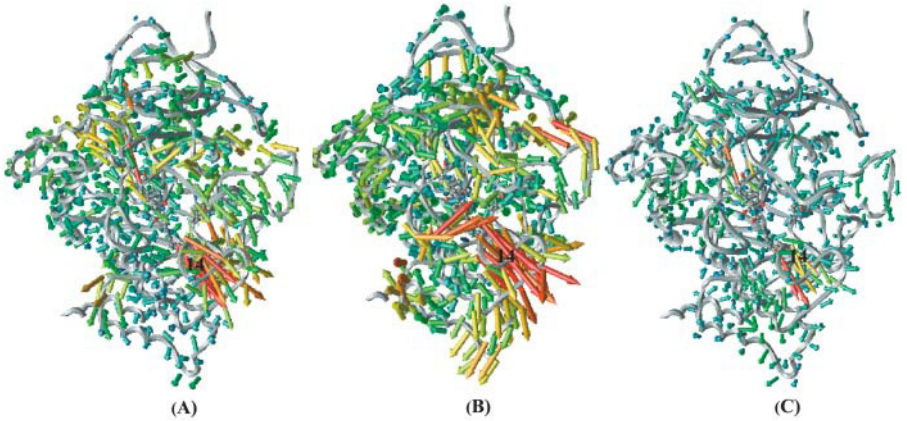

FIGURE 5 Porcupine plots showing the collective motions of the protein at different TMA positions. (*A*) The pre-crossing: the TMA is at the position 10.0 Å before it crosses the barrier peak. (*B*) The transition: the TMA is at peak of the PMF 11.3 Å. (*C*) The postcrossing: the TMA stays at 13.5 Å, after it passes through the barrier. Correlation parameters of the C_α atoms are averaged over the 12 full MD trajectories data set. In each, the view is down into the gorge, and Y124 (*top*), F338 (*bottom*), and S203 (*middle right*) are shown in ball-and-stick representations; the numeral 14 is used to indicate the location of helix 14.

motion of the protein for the three different TMA positions. It clearly illustrates that large portions of the enzyme move in a concerted fashion to contribute to the opening and closing events. When the gorge is widely open, many residues dilate radially from the gorge axis, helping to open the bottleneck. In particular, the main contribution to widening the bottleneck comes from helix 14, which lines the gorge on the lower right in Fig. 5 *B*. This same helix was also observed to move when the gorge opened in the study by Tai et al. (2001). In contrast, after the TMA crosses the barrier, the protein relaxes toward its original state; in Fig. 5 *C*, the vectors are mostly in blue. These results demonstrate that both side chains and backbone motions contribute to the opening of the gorge and facilitate the passage of the TMA.

CONCLUSION

The aromatic residues that line the gorge seem not only to facilitate the movement of the cation in the gorge through π-cation interaction (Sussman et al., 1991), but also may serve to enable fast switching between the open and closed states (McCammon et al., 1983; Zhou et al., 1998). Small and fast fluctuations of the aromatic side chains in this bottleneck region, together with the backbone displacements containing residues Y124 and F338 contribute on the picosecond timescale. The larger scale collective motions of the enzyme that are coupled with the movement of the ligand through the bottleneck region are expected to be important for the binding of ligands larger than ACh in the active site. The simple umbrella sampling method used here could be complemented by other types of simulation to further characterize the gating mechanism (Bolhuis et al., 2002; Gullingsrud et al., 2001; Huo and Straub, 1997; Israelewitz et al., 2001; Olender and Elber, 1996). The low energy barrier in the bottleneck region obtained from this study is consistent with experimental data indicating the enzyme operates in the diffusion-controlled limit, despite the fact that the bulky side chains of the aromatic residues would seem to hinder the motion of the ligand.

J.B. thanks Dr. Kaihsu Tai at the University of Oxford and Dr. Jung-Hsin Lin at the National Taiwan University for initial setup assistance and invaluable discussion. J.B. also thanks Mr. Andreas Vitalis for help with programming techniques. We also thank Dr. Tjerk Straatsma at the Pacific Northwest National Laboratory for umbrella sampling technical support.

This project was supported in part by the National Institutes of Health, the National Science Foundation, the National Biomedical Computation Resource, the Howard Hughes Medical Institute, the San Diego Supercomputer Center, National Science Foundation Center for Theoretical Biological Physics, and Accelrys, Inc.

REFERENCES

Antosiewicz, J., S. T. Wlodek, and J. A. McCammon. 1996. Acetylcholinesterase: role of the enzyme's charge distribution in steering charged ligands toward the active site. *Biopolymers*. 39:85–94.

Bolhuis, P. G., D. Chandler, C. Dellago, and P. L. Geissler. 2002. Transition path sampling: throwing ropes over rough mountain passes, in the dark. *Annu. Rev. Phys. Chem.* 53:291–318.

Bourne, Y., P. Taylor, and P. Marchot. 1995. Acetylcholinesterase inhibition by fasciculin-crystal-structure of the complex. *Cell.* 83:503–512.

Case, D. A. 1993. Computer-simulations of protein dynamics and thermodynamics. *Computer*. 26:47–57.

Cornell, W. D., P. Cieplak, C. I. Bayly, I. R. Gould, K. M. Merz, D. M. Ferguson, D. C. Spellmeyer, T. Fox, J. W. Caldwell, and P. A. Kollman. 1995. A second generation force field for the simulation of proteins, nucleic acids, and organic molecules. *J. Am. Chem. Soc.* 117:5179–5197.

Enyedy, I. J., I. M. Kovach, and B. R. Brooks. 1998. Alternate pathways for acetic acid and acetate ion release from acetylcholinesterase: a molecular dynamics study. *J. Am. Chem. Soc.* 120:8043–8050.

Faerman, C. H., D. R. Ripoll, I. Silman, and J. Sussman. 1993. An electrostatic mechanism of substrate recognition by acetylcholinesterase. *J. Cell. Biochem.* 230–230.

Gilson, M. K., T. P. Straatsma, J. A. McCammon, D. R. Ripoll, C. H. Faerman, P. H. Axelsen, I. Silman, and J. L. Sussman. 1994. Open back door in a molecular-dynamics simulation of acetylcholinesterase. *Science*. 263:1276–1278.

Gullingsrud, J., D. Kosztin, and K. Schulten. 2001. Structural determinants of MscL gating studied by molecular dynamics simulations. *Biophys. J.* 80:2074–2081.

Hanggi, P., P. Talkner, and M. Borkovec. 1990. Reaction-rate theory—50 years after Kramers. *Rev. Mod. Phys.* 62:251–341.

Hosea, N. A., Z. Radic, I. Tsigelny, H. A. Berman, D. M. Quinn, and P. Taylor. 1996. Aspartate 74 as a primary determinant in acetylcholinesterase governing specificity to cationic organophosphonates. *Biochemistry*. 35:10995–11004.

Humphrey, W. A. D., and K. Schulten. 1996. Visual molecular dynamics. *J. Mol. Graph.* 14:33–38.

Huo, S. H., and J. E. Straub. 1997. The maxflux algorithm for calculating variationally optimized reaction paths for conformational transitions in many body systems at finite temperature. *J. Chem. Phys.* 107: 5000–5006.

Israelewitz, B., J. Baudry, J. Gullingsrud, D. Kosztin, and K. Schulten. 2001. Steered molecular dynamics investigations of protein function. *J. Mol. Graph.* 19:13–25.

Kottalam, J., and D. A. Case. 1988. Dynamics of ligand escape from the heme pocket of myoglobin. *J. Am. Chem. Soc.* 110:7690–7697.

Malany, S., N. Baker, M. Verweyst, R. Medhekar, D. M. Quinn, B. Velan, C. Kronman, and A. Shafferman. 1999. Theoretical and experimental investigations of electrostatic effects on acetylcholinesterase catalysis and inhibition. *Chem. Biol. Interact.* 120:99–110.

Mallender, W. D., T. Szegletes, and T. L. Rosenberry. 2000. Acetylthiocholine binds to ASP74 at the peripheral site of human acetylcholinesterase as the first step in the catalytic pathway. *Biochemistry.* 39:7753–7763.

Marrink, S. J., and H. J. C. Berendsen. 1996. Permeation process of small molecules across lipid membranes studied by molecular dynamics simulations. *J. Phys. Chem.* 100:16729–16738.

McCammon, J. A., and S. C. Harvey. 1987. Dynamics of proteins and nucleic acids. Cambridge University Press. New York.

McCammon, J. A., C. Y. Lee, and S. H. Northrup. 1983. Side-chain rotational isomerization in proteins - a mechanism involving gating and transient packing defects. *J. Am. Chem. Soc.* 105:2232–2237.

Northrup, S. H., M. R. Pear, C. Y. Lee, J. A. McCammon, and M. Karplus. 1982. Dynamical theory of activated processes in globular-proteins. *Proc. Natl. Acad. Sci. USA.* 79:4035–4039.

Olender, R., and R. Elber. 1996. Calculation of classical trajectories with a very large time step: Formalism and numerical examples. *J. Chem. Phys.* 105:9299–9315.

Quinn, D. M. 1987. Acetylcholinesterase - enzyme structure, reaction dynamics, and virtual transition-states. *Chem. Rev.* 87:955–979.

Radic, Z., P. D. Kirchhoff, D. M. Quinn, J. A. McCammon, and P. Taylor. 1997. Electrostatic influence on the kinetics of ligand binding to acetylcholinesterase. Distinctions between active center ligands and fasciculin. *J. Biol. Chem.* 272:23265–23277.

Ripoll, D. R., C. H. Faerman, P. H. Axelsen, I. Silman, and J. L. Sussman. 1993. An electrostatic mechanism for substrate guidance down the aromatic gorge of acetylcholinesterase. *Proc. Natl. Acad. Sci. USA.* 90:5128–5132.

Roux, B., and M. Karplus. 1991a. Ion-transport in a gramicidin-like channel—dynamics and mobility. *J. Phys. Chem.* 95:4856–4868.

Roux, B., and M. Karplus. 1991b. Ion-transport in a model gramicidin channel—structure and thermodynamics. *Biophys. J.* 59:961–981.

Shen, J., and J. A. McCammon. 1991. Molecular-dynamics simulation of superoxide interacting with superoxide-dismutase. *Chem. Phys.* 158: 191–198.

Straatsma, T. P., M. Philippopoulos, and J. A. McCammon. 2000. NWChem: exploiting parallelism in molecular simulations. *Comput. Phys. Commun.* 128:377–385.

Sussman, J. L., M. Harel, F. Frolow, C. Oefner, A. Goldman, L. Toker, and I. Silman. 1991. Atomic-structure of acetylcholinesterase from *Torpedo californic*a—a prototypic acetylcholine-binding protein. *Science.* 253: 872–879.

Tai, K., T. Y. Shen, U. Borjesson, M. Philippopoulos, and J. A. McCammon. 2001. Analysis of a 10-ns molecular dynamics simulation of mouse acetylcholinesterase. *Biophys. J.* 81:715–724.

Tai, K. S., T. Y. Shen, R. H. Henchman, Y. Bourne, P. Marchot, and J. A. McCammon. 2002. Mechanism of acetylcholinesterase inhibition by fasciculin: A 5 ns molecular dynamics simulation. *J. Am. Chem. Soc.* 124:6153–6161.

Tan, R. C., T. N. Truong, J. A. McCammon, and J. L. Sussman. 1993. Acetylcholinesterase - electrostatic steering increases the rate of ligand-binding. *Biochemistry.* 32:401–403.

Wlodek, S. T., J. Antosiewicz, and J. M. Briggs. 1997. On the mechanism of acetylcholinesterase action: The electrostatically induced acceleration of the catalytic acylation step. *J. Am. Chem. Soc.* 119:8159–8165.

Wlodek, S. T., T. Y. Shen, and J. A. McCammon. 2000. Electrostatic steering of substrate to acetylcholinesterase: Analysis of field fluctuations. *Biopolymers.* 53:265–271.

Wong, Y. T., T. W. Clark, J. Shen, and J. A. McCammon. 1993. Molecular-dynamics simulation of substrate-enzyme interactions in the active-site channel of superoxide-dismutase. *Molecular Simulation.* 10:277–289.

Zhou, H. X., S. T. Wlodek, and J. A. McCammon. 1998. Conformation gating as a mechanism for enzyme specificity. *Proc. Natl. Acad. Sci. USA.* 95:9280–9283.